Particle Filter Prognostic Applied in Landing Gear Retraction

Paula Borges Olivio Cerdeira[1], Roberto Kawakami Harrop Galvão[2] and João Pedro Pinheiro Malère[1]

[1] *EMBRAER S.A., São José dos Campos, São Paulo, 12227-901, Brazil*

paula.olivio@embraer.com.br
joao.malere@embraer.com.br

[2] *ITA – Instituto Tecnológico de Aeronáutica, São José dos Campos, São Paulo, 12228-900, Brazil*

kawakami@ita.br

ABSTRACT

The PHM (Prognostics and Health Monitoring) applications play an increasingly important role on the aeronautical industry and can provide a wide range of benefits for complex systems, such as aircraft landing gears (LDG). Indeed forecasting the RUL (Remaining Useful Life) of the landing gear subsystems can enable condition–based maintenance, improve the aircraft availability and reduce unscheduled events. The purpose of this work is to investigate nominal and degraded simulated retraction times of a landing gear and to apply a prognostics approach, specifically the particle filter (PF) algorithm, from which the RUL can be predicted at a given confidence level.

1. INTRODUCTION

The future vision for complex systems, such as an aircraft, is the self-monitoring and control. The exploitation of Prognostics and Health Monitoring (PHM) may lead to important competitive advantages in terms of maintenance and operations (ACARE, 2010). Over the past years, the health monitoring community has vastly extended its capability to monitor systems for the improvements on forecasting and prediction (Khuzadi, 2008).

Many authors have already discussed about new paradigms for product life-cycle support. Camci, Valentine & Navarra (2007), Papakostas et al, (2010), Kalgren et al (2007) and Rodrigues, Yoneyama & Nascimento (2012) label the importance of the PHM use in aeronautical maintenance and for the decision making, by enabling effectiveness on troubleshooting, improved logistics and increased fleet availability. In other words PHM is the basis for decision support in a complex environment enabling better planning and subsequently boosting operational availability.

Figure 1 illustrates the estimation of degradation for a system being monitored and the approximation for the system RUL as a probability density function (PDF).

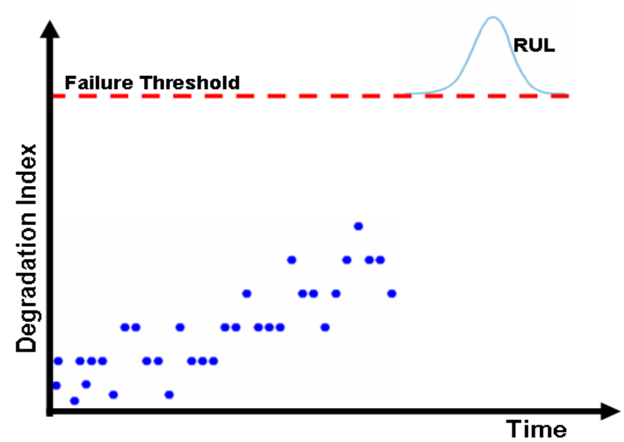

Figure 1. RUL estimation

Large complex systems such as aircraft landing gears (LDG) are composed of multiple systems and subsystems. LDG plays an important role in aircraft safety, comfort and stability. Some examples for the LDG failure modes are the blocked circuit, degraded seals, leak and vibration (Oliva et al, 2012). The aircraft LDG health monitoring may improve the aircraft dispatchability and the operational efficiency, avoiding unscheduled maintenance, Aircraft-on-Ground (AOG) events and other impacts. One example was the crash on July 2013 of the flight 345 due to nose LDG collapse during landing at LaGuardia Airport (AIRNATION.NET).

Ji, Zhang & Dong (2011) studied the LDG retraction and extension problem and the operational impact of some components degradation. Zhou, Yunxia and Rui (2011) modeled the LDG dynamics and studied structural problems occurred by the effect of the hard landing and suggested the adoption of PHM solution for this issue.

The present work is composed by a PF algorithm for the landing gear retraction subsystem in order to estimate its RUL. A computational model proposed by Denery et al (2006) was used to simulate the dynamics and different degradation conditions of the LDG retraction subsystem.

Regarding Particle Filter (PF), it is considered state of the art in nonlinear non-Gaussian state estimation (NASA; Orchard; Vachtsevanos et al, 2006).Goebel et al (2008) made a comparison between PF and other regression methods for a battery health management, and concluded that PF is a sophisticated technique considering the accuracy for the smaller estimations. Saha & Goebel (2009) modeled Li-ion battery capacity depletion by the use of PF framework for the predictions of the EOD (end-of-discharge) and EOL (end-of-life) effectively.

This paper is organized as follow: in Section 2, a brief description of the landing gear retraction model is presented; in Section 3, the PF algorithm is explained, in Section 4 the simulation and the estimation results are discussed, followed by conclusions in Section 5.

2. Landing Gear Simulation Model

The first step for the generation of landing gear data was the reuse of an existing Landing Gear (LDG) model proposed by Denery et al (2006). The reused model is a faithful description of the right main LDG of HL20 aircraft in terms of physical representation. It was implemented in Simulink® using some blocks of the SimMechanics® tool.

Figure 2 presents the Simulink block diagram employed in the LDG model simulations.

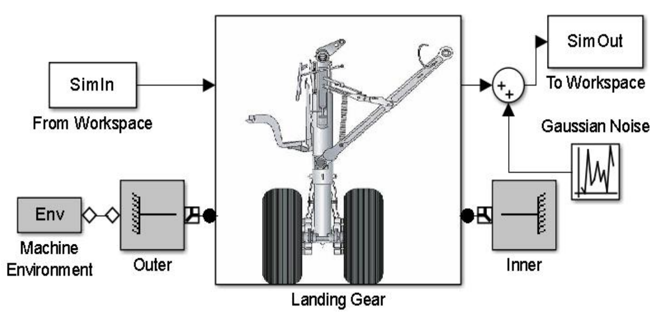

Figure 2. LDG Model

We included three special blocks on the model shown in Figure 2, compared to the original file: SimIn, SimOut and Gaussian Noise.

The SimIn block represents the landing gear actuator force and it was used to introduce degradation effects.

Gaussian noise block was added to simulate imperfections in the angular displacement measurements.

The results of each simulation were stored in the Matlab workspace by using the SimOut block.

The blocks in gray are from the original model, the Inner and Outer blocks represent the aircraft structure restrictions and the Env block controls the environment, including dynamic simulation, gravity, tolerance and restrictions of the movement modes. None of the parameters inside these blocks was changed.

2.1. Input Model

Figure 3 represents the actuator input force over LDG cycles, representing the system degradation, due to loss of hydraulic pressure, for example. Each cycle corresponds to a LDG retraction. An initial nominal force retraction of 5600N was defined and in every step a random value between 0N and -50N was added.

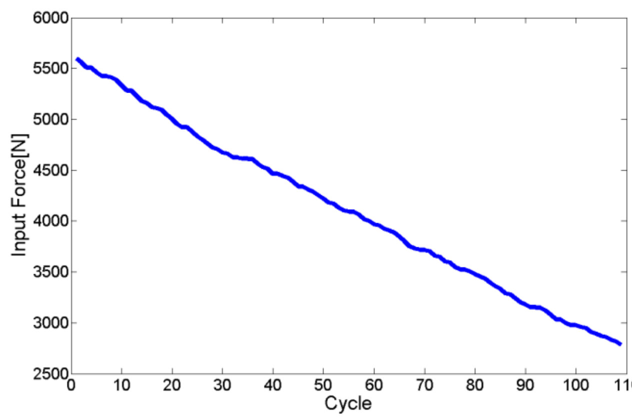

Figure 3. Input Force

The decreasing actuator input force may be associated with some failures modes. Some data observed at field events indicates linear loss of hydraulic pressure, degraded seals or valves and clogged hydraulic lines. Based on this field empirical data, the profile shown on Figure 3 was considered in this study.

2.2. LDG simulation

The LDG model outputs the retraction angle, however an algorithm takes into account this output in order to define the LDG retraction time. In this study it was defined the retraction angle that indicates the maximum degradation effect correlated to the retraction time.

The first simulation step was to establish an index, as shown in equation (1). A similar function is described by Azimi-Sadjadi et al (2000) as an uncorrelated-features assumption by the Fisher discriminant function, which in this case is used to define the angle that maximizes the degradation effect:

$$I = \left. \frac{(\mu_D - \mu_N)^2}{\sigma_D^2 + \sigma_N^2} \right|_{n=30} \tag{1}$$

where $\mathbf{\mu_D}$ is the mean retraction time of a set of simulations for each input force, $\mathbf{\mu_N}$ mean nominal retraction time, $\mathbf{\sigma_D}$ degraded retraction time standard deviation, $\mathbf{\sigma_N}$ nominal retraction standard deviation, **I** degradation index, ***n*** number of simulations. Figure 4(a) represents the LDG retraction simulation for the nominal input force, and shows the mean and the standard deviation of the retraction times between 0 and 70 degrees. Figure 4(b) illustrates the LDG retraction simulation with a degraded input force with the mean retraction time and the standard deviation.

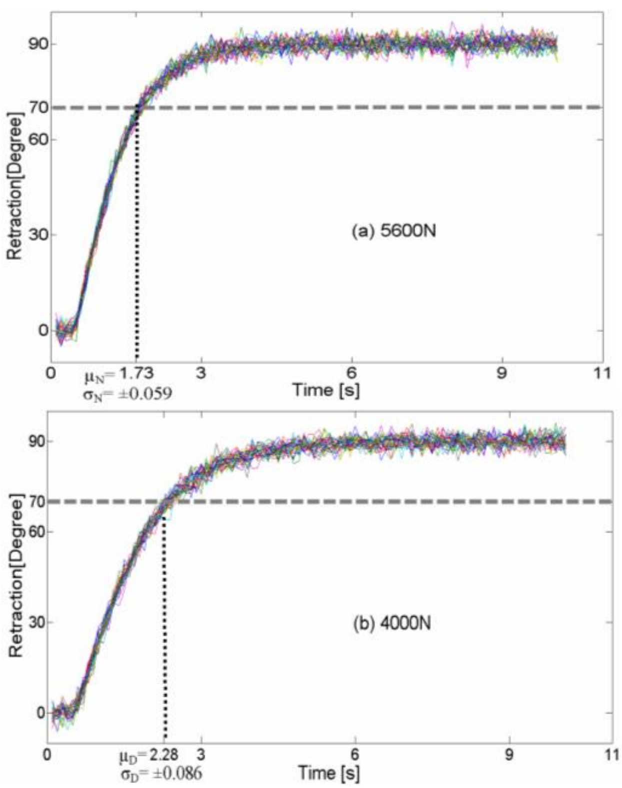

Figure 4. Comparison Simulation for LDG Retraction

Figure 4(b) shows slower retraction times than the ones shown in Figure 4 (a), what illustrates the degradation.

In order to get the best angular displacement which represents the maximum degradation index, four input forces were defined (4000N, 4500N, 5000N and 5600N). Arbitrarily, it was decided that the nominal force was 5600N and the considered degraded conditions were with forces of 5000N, 4500N and 4000N. Note that the model retraction starts with 0° and stops with 90°.

We found reasonable 30 simulations for each input force and a comparison was made among the μ and σ of the nominal force and the degraded ones, as represented in equation (1). According to the results, the 70 degrees presented the maximum index. In other words, the degradation index was established as being the retraction time from 0 to 70 degrees. Figure 5 illustrates the output of the first part of the simulation step results.

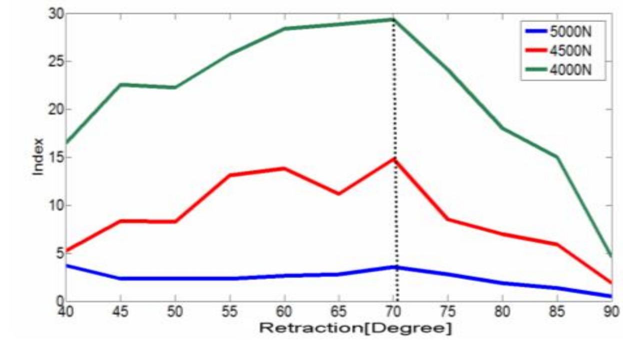

Figure 5. Best Index for Angular Displacement

The second step was to find the failure threshold. We had established the 3000N force as the minimum input force and set 30 simulations in order to get the μ for the failure retraction time and it was around 2.93 seconds. This result is the threshold input for the PF algorithm, to be detailed in Section 4.1. Note that the 3000N force was adopted as being the minimum force needed to perform the LDG retraction.

Finally, the simulations were performed with an initial actuator force and decreased by a delta random force value. The results of the LDG retraction time simulation were recorded to be used on the PF algorithm.

Table 1 shows the initial parameters used in LDG model.

Table 1. LDG Simulation Parameters

Parameter	Value	Unit
Gaussian Noise Mean	0	Degree
Gaussian Noise standard deviation	2	Degree
Time sampling	0.1	Second
Total Simulation time	10	Second
Initial Actuator Force	5600	Newton
Delta Force	(0,-50)	Newton

Figure 6 illustrates the steps of the landing gear simulation.

Figure 6. Schematic of LDG Simulations

3. Particle Filter

Particle Filter in model-based prognostics utilizes a concept of sequential importance sampling and Bayesian theory.

The PF algorithm involves prediction and filtering steps. The prediction step uses both previous state and the process model to generate an a priori probability density function (PDF) for the state at the next time instant, as shown in equation (2).

$$P(x_k \mid z_{1:k-1}) = \int P(x_k \mid x_{k-1}) P(x_{k-1} \mid z_{1:k-1}) dx_{k-1} \quad (2)$$

The filtering step considers the current observations Z_k and the a priori PDF to generate the posteriori state PDF, using Bayes' formula as shown in equation (3).

$$P(x_k \mid z_{1:k}) = \frac{P(z_k \mid x_k) P(x_k \mid z_{1:k-1})}{P(z_k \mid z_{1:k-1})} \quad (3)$$

The core idea is to construct a PDF of the state based on all available information. For nonlinear systems the particles are generated and recursively updated from a nonlinear process model that describes the evolution in time, in this case on each cycle, under analysis of a measurement (Z_k) and the *priori* estimate of the state PDF (Goebel et al., 2008).

Figure 7 summarizes the landing gear PF flowchart. The prediction parameters utilize the damage state model, as shown in equation (4), for prediction and filtering step.

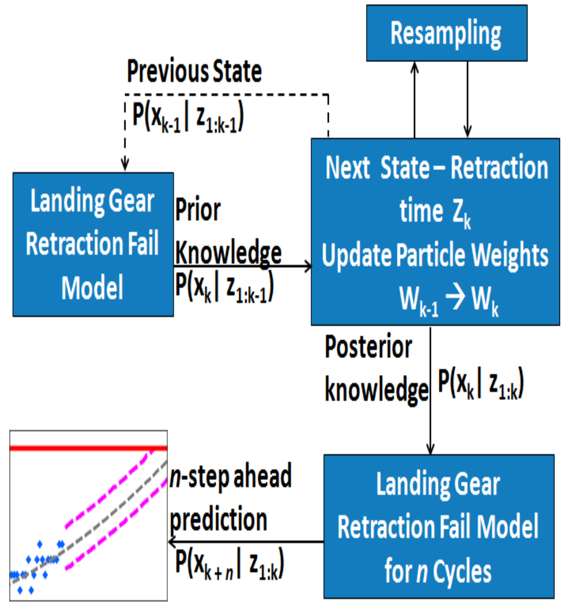

Figure 7. Particle Filter Flowchart

The landing gear retraction fail model is an empirical function, that can be written recursively in terms of the previous step, and it was obtained from the simulation measurements. It is represented in equation (4):

$$x(k) = ae^{bk} \quad (4)$$

where $x(k)$ is the prediction parameter (LDG retraction time) of k cycles. The coefficients *a* and *b* represents the exponential damage state. More details about this model can be found in Section 4.1.

The particles are generated and updated from the *prior knowledge* of the state PDF, then propagated through landing gear cycles using the nonlinear equation (4) which is recursively updated by using the observed data (measurements). The algorithm than continues with the propagation of the particles until the failure threshold to give the RUL PDF.

Figure 8 summarizes one step for PF algorithm cycle adapted from An, Choi & Kim (2012).

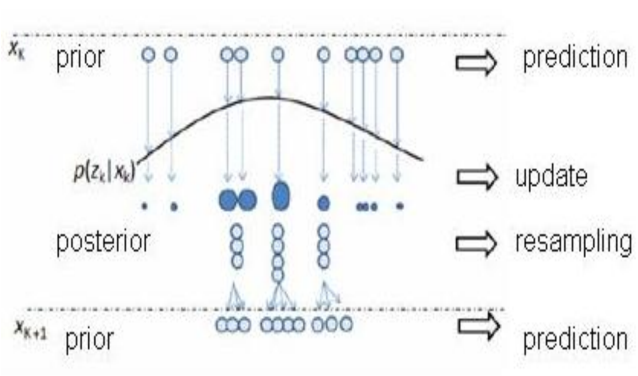

Figure 8. PF algorithm steps

4. SIMULATION

4.1. Simulation scenario

The LDG model described on section 2 was used to simulate the retraction times given the Gaussian noise (Figure 2) and the degradation profile (Figure 3) We established 60 points as observed data (Z_k). Figure 9 shows the measure values and the retraction time failure threshold.

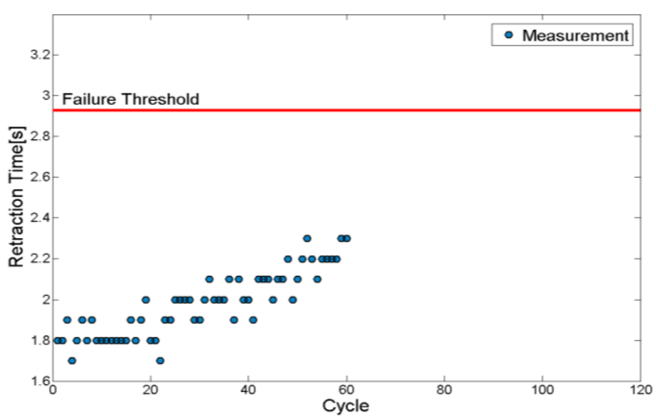

Figure 9. Retraction Time Measurement

The initial estimations for the coefficients b_0 in equation (4) were found by fitting an exponential function through the measurement values. It was adjusted in a C.I. to accommodate the samples inside it.

The initial damage value x_0 was set with the same initial value as the a_0.

Figure 10 shows the polynomial curve, as well as the confidence interval.

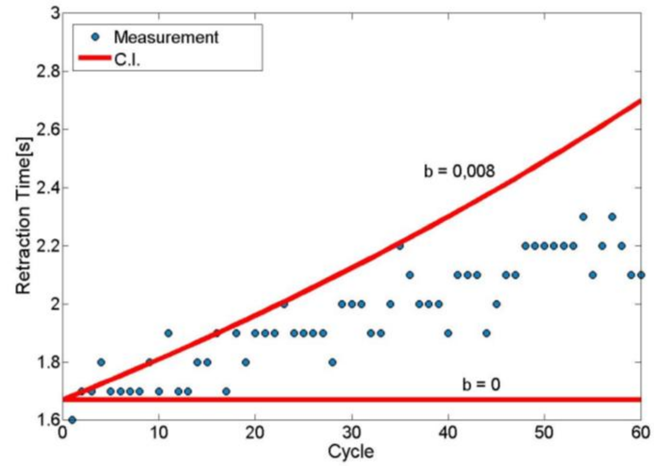

Figure 10. Exponential fitting

Table 2 shows the parameters of this first simulation considering 0.1s for the time sampling. U(α_{min},α_{max}) denotes a uniform probability density function with support [α_{min},α_{max}].

Table 2. PF Simulation Parameters

Parameter	Value	Unit
Threshold	2.93	Second
Particles	10e3	
Significance Level C.I.	95%	
Initial Damage x_0	U(1.6,1.9)	Second
Initial Parameter b_0	U(0,0.008)	
Initial Std Deviation of Measurement Error s_0	U(0,0820, 0,0902)	Second

The distribution of the standard deviation measurement error was obtained by the examination of the first 20 measure values of the LDG retraction time in a bootstrap procedure.

More two scenarios were simulated with different time sampling 0.05s and 0.2s, following the same steps as described in Section 2.2. Table 3 shows the parameters for different time sampling simulation.

Table 3. PF Simulation Parameters

Parameter	Value (0,05s)	Values (0,2s)	Unit
Threshold	2,33	2,8	Second
Initial Damage x_0	U(1,35, 1,55)	U(1,6, 1,8)	Second
Initial Parameter b_0	U(0, 0,008)	U(0, 0,008)	
Initial Std Deviation of Measurement Error s_0	U(0,0579, 0,0636)	U(0,0838, 0,0905)	Second

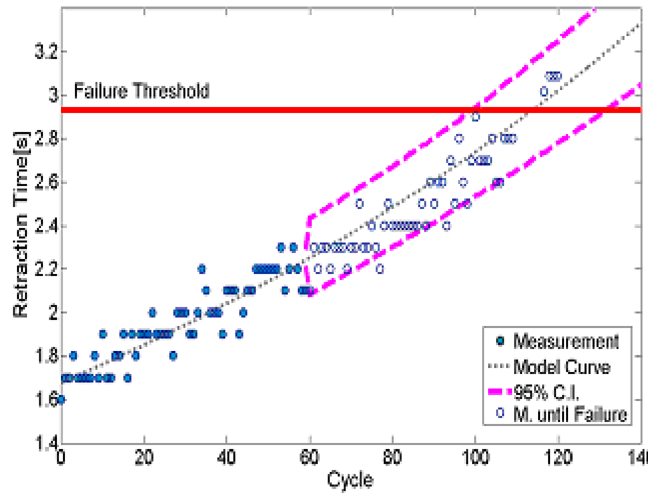

Figure 12. PF Predictions versus Measurement

4.2. Simulation Results

After defining the parameters, we ran a set of simulations adjusting the significance level and compared results with true simulated data until the failure threshold.

The estimation of the RUL for the first simulated scenario, considering the 0.1s as time sampling, resulted on a median value around cycle 49 and the interval considering the significance level was between cycles 40 and 60.

We can observe in Figure 12 the predicted future damage states, which were obtained by propagating the particles though the damage model until it reaches the Failure Threshold.

Figure 12 shows the predictions of the LDG retraction time and true simulated data after cycle 60 until the failure threshold. Most of the data fits inside the prediction interval of the PF.

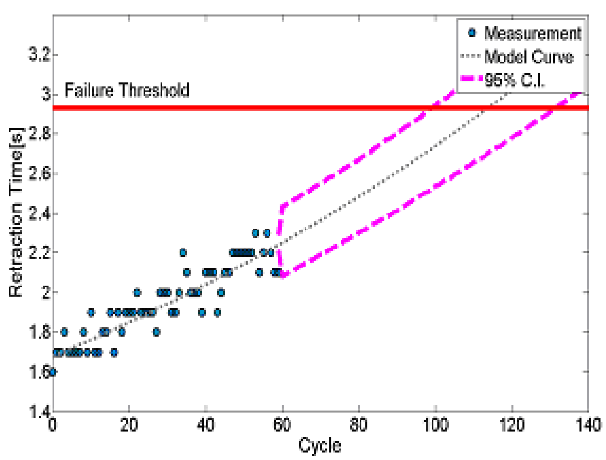

Figure 11. PF Predictions

A set of simulations were done using different time sampling in other to demonstrate how this parameter can interfere into the precision of the RUL. Figure 13 indicates the estimation for 0.05s time sampling and Figure 14 indicates the estimation for 0.2s time sampling.

Figure 13 shows a predicted growth rate slightly steeper and a lower dispersion with respect to the model curve when compared to the Figure 14. This analysis indicates greater dispersion between the values for samples of 0.2s and RUL forward in time.

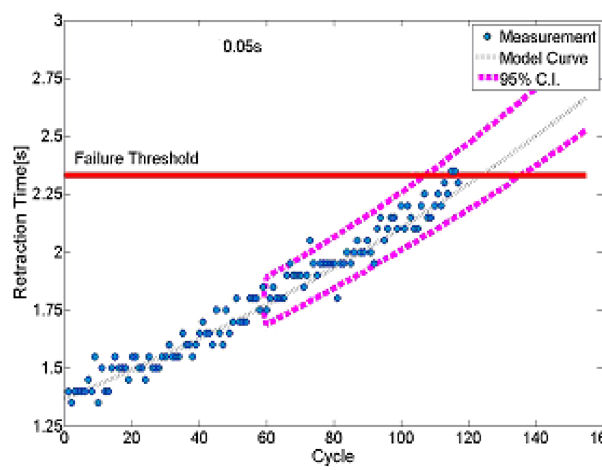

Figure 13. Estimation for 0.05s Time Sampling

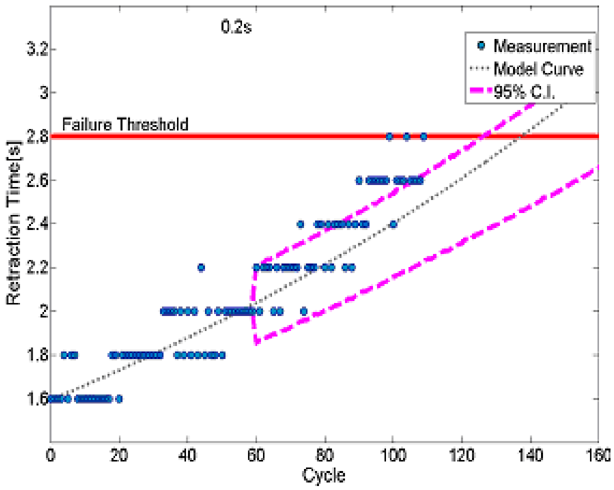

Figure 14. Estimation for 0.2s Time Sampling

Through Figure 15 we can make a comparison between the RUL for the three different time sampling simulations (0.05s, 0.1s and 0.2s). It can be noticed that the higher the interval between samplings (0.2s), the higher is the standard deviation as one can see the measurements outside the C.I crossing the failure threshold in Figure 14.

The estimated failure mean cycle for the time sampling 0.05s, 0.1s and 0.2s is 55 °, 49 ° and 79°, respectively, and the standard deviation is 6.18, 6.36 and 9.39. In this study the time sampling of 0.2s is inappropriate since the failure occurs before the estimation of the RUL.

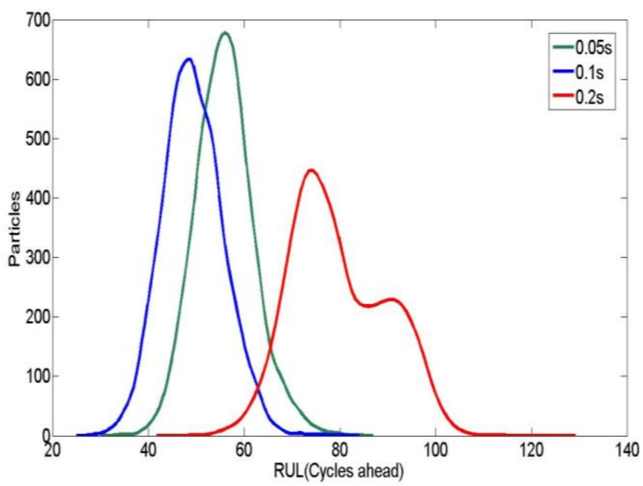

Figure 15. RUL for Different Sampling Times

5. Conclusions

This paper presented a method to obtain the remaining useful life for the landing gear retraction subsystem, based on PF techniques for estimation.

A landing gear model was used to simulate the system dynamic behavior and adapted to establish the degradation index. For the failure mode under investigation a model was presented based on the simulated data.

The results obtained by simulating the PF algorithm with measured values from the LDG model allowed a reasonable prediction level against the true data for the 0.05s and 0.1s time sampling. However the 0.2s time sampling is considered inappropriate for the remaining life prediction.

Future research may extend the proposed models for the LDG extension. To mature the algorithm, aircraft raw data may be analyzed using the PF algorithm. Finally other opportunity could include the comparison of the prediction interval using a different PHM approach.

Acknowledgment

The authors acknowledge the support of FAPESP (grant 2011/17610-0) and CNPq (research fellowship).

References

ACARE << (Advisory Council for Aeronautics Research in Europe), et al. Aeronautics and Air Transport: Beyond Vision 2020 (Towards 2050). 2010>>, http://ec.europa.eu/research/transport/pdf/acare_background_2010_en.pdf, accessed 02/02/2013.

An, D., Choi, J.H. & Kim, N. (2013). Prognostics 101: A Tutorial for Particle Filter-Based Prognostics Algorithms Using Matlab. *Reliability Engineering and System Safety*, vol. 115, pp. 161-169.

Airnation.net<<NTSB Issues Update into Southwest Flight 345 Accident at LaGuardia Airport in New York>>, http://airnation.net/2013/07/26/ntsb-southwest-345-update, accessed 09/03/2013.

Azimi-Sadjadi, M.R. et al. Underwater target classification using wavelet packets and neural networks. *IEEE Transactions on Neural Networks*, vol. 11. n.3, 2000.

Camci, F., Valentine, G., Navarra, K. (2007). Methodologies for Integration of PHM System with Maintenance Data. *IEEE Aerospace Conference,* Big Sky.

Denery, T., et al. (2006). Creating Flight Simulator Landing Gear Models Using Multidomain Modeling Tools. *The MathWorks, Inc.*

Goebel, K., et al. (2008). Prognostics in Battery Health Management. *IEEE Instrumentation and Measurements Magazine, vol. 11(4), pp.33-40.*

Ji, G., Zhang, L. & Dong M. (2011). Dynamic simulation on retraction\ extension system of an aircraft. *Proceedings of Prognostics and System Health Management*

Conference, Shenzhen.

Kalgren, P., et al. (2006). Defining PHM, a lexical evolution of maintenance and logistics. *IEEE Aerospace Conference,* Big Sky.

Khuzadi, M. (2008). On Health Monitoring. *IEEE Aerospace Conference,* Big Sky.

Nasa,« Batteries Prognostic - Particle Filtering», http://ti.arc.nasa.gov/tech/dash/pcoe/battery-prognostics/algorithms/ , accessed 05/11/2013.

Oliva, G. M., et al. (2012). Prognostics Assessment Using Fleet-wide Ontology. *Proceedings of International Conference on Prognostics and Health Management,* Minneapolis.

Orchard, M. & Vachtsevanos, G. (2009). A Particle Filtering Approach for Online Fault Diagnosis and Failure Prognosis. Transactions of the Institute of Measurement and Control, no. 3-4, p. 221–246.

Papakostas, N. et al. (2010). An Approach to Operational Aircraft Maintenance Planning. Decision Support Systems, Vol. 48, Issue 4, Elsevier Science Publishers B.

Rodrigues, L. R., Yoneyama, T. & Nascimento Jr., C. L. (2012). How Aircraft Operators Can Benefit from PHM Techniques. *IEEE Aerospace Conference,* Big Sky.

Saha, B. & Goebel, K. (2009). Modeling Li-Ion battery capacity depletion in a particle filtering framework. *Proceedings of International Conference on Prognostics and Health Management,* San Diego.

Vachtsevanos, G., Lewis, F.L., Roemer, M., Hess, A., & Wu, B. (2006). *Intelligent Fault Diagnosis and Prognosis for Engineering Systems.* Hoboken, NJ: John Wiley & Sons, Inc

Zhou, Y., Yunxia, C. & Rui, K. (2011). A Study of Aircraft Landing Gear Testing System on PHM. *Prognostics and System Health Management Conference, Shenzhen.*

BIOGRAPHIES

Paula Borges Olivio Cerdeira holds a bachelor's degree in Computer Engineering from Centro Universitário e Fundação Santo André (FSA, 2007), Brazil. She is currently pursuing her Master Degree in Aeronautical Engineering from Instituto Tecnológico de Aeronáutica at ITA. She is with EMBRAER S.A. São José dos Campos, São Paulo, Brazil, since 2011. She works as a Development Engineer in an R&T group at EMBRAER performing research on IVHM technology for application to aeronautical systems. Her current research interests are the application of health monitoring techniques for systems and the usage of PHM information for decision making.

Roberto Kawakami Harrop Galvão is an Associate Professor of Systems and Control at the Electronic Engineering Department of ITA. He holds a bachelor's degree in Electronic Engineering (Summa cum Laude, 1995) from Instituto Tecnológico de Aeronáutica (ITA), Brazil. He also obtained the master's (1997) and doctorate (1999) degrees in Systems and Control from the same institution. Since 1998 he has been with the Electronic Engineering Department of ITA as a full-time academic. Dr. Galvão is a Senior Member of the IEEE and an Associate Member of the Brazilian Academy of Sciences. He has published more than 200 papers in peer-reviewed journals and conference proceedings. His main areas of interest are fault diagnosis and prognosis, wavelet theory and applications, and model predictive control.

João Pedro Pinheiro Malère holds a bachelor's degree in Control Engineering from Universidade Estadual de Campinas (Unicamp, 2004), Brazil, and a Master Degree in Aeronautical Engineering from Instituto Tecnológico de Aeronáutica (ITA, 2007), São José dos Campos, São Paulo, Brazil. He is with EMBRAER S.A., São José dos Campos, São Paulo, Brazil, since 2006. He works as a Development Engineer in an R&T group at EMBRAER performing research on IVHM technology for application to aeronautical systems. His current research interest is on integrated health management systems.